East European Journal of Physics. 3. 236-247 (2024)
DOI:10.26565/2312-4334-2024-3-23 ISSN 2312-4334

MHD STEFAN FLOW OF CASSON NANOFLUID COMPLETES A POROUS MEDIUM IN THE PRESENCE OF CHEMICAL REACTION WITH THE EFFECT OF THOMPSON AS WELL AS - TROIAN SLIP OVER A PLATE IN THE COMPANY OF RADIATION

Anitha Deevi Reddy[a], Prabhakara Reddy Deevi Reddy[a], Bhagya Lakshmi Kuntumalla[b], Sneha Latha Madhura[c,d], Parandhama Areti[e]*

[a]Mathematics and Computing skills unit, Preparatory Studies Centre, University of Technology and Applied Sciences – Nizwa, Sultanate of Oman – 611
[b]Department of Mathematics, CMR Technical Campus, Medchal, Hyderabad, Telangana -501401, India
[c]Department of Mathematics, Sambhram Academy of Management Studies, Bangalore-560097, India
[d]Sambhram University, Jizzax, Uzbekistan-130100
[e]Department of Mathematics, Institute of Aeronautical Engineering, Hyderabad, Telangana-500043, India
**Corresponding Author e-mail: a.parandhama@iare.ac.in*
Received May 22, 2024; revised July 9, 2024; accepted July 12, 2024

In this work, we report the effects of Thompson, Troian slip, and Stefan blowing on the magnetohydrodynamic (MHD) Cassonnanofluid behavior via a porous media while a chemical reaction is taking place. We also examine the effects of radiation parameters, Joel heat, and velocity distribution using a two-phase model for nanofluids. Similarity transformations may be used to convert the primary Partial Differential Equations (PDEs) into Ordinary Differential Equations (ODEs). MATLAB Shooting and Runge-Kutta algorithms may be used to solve nonlinear equations. The variations in non-dimensional parameters show the effects on mass transfer, heat, and fluid flow properties. It is shown that the skin friction coefficient falls as the Stefan blowing parameter S increases. As the values of the Thompson and Troian slip parameters increase, the fluid concentration decreases. With an increase in Nt, Nb, and k, the fluid's heat rises but its concentration falls. The results of this analysis provide several enticing aspects that are going to give merits for further study of the problems.
Keywords: *Casson; Chemical reaction; MHD; Porous; Radiation; Thompson and Troian slip*
PACS: 52.30.Cv, 61.30.Pq, 83.10.Bb

1. INTRODUCTION

For the past few decades, the study of nanofluids has been a desirous investigation. Nanofluids are used in a wide range of fields, including research, geophysics, biomedicine, chemical engineering, and electronic cooling. The first to propose the concept of "nanofluid" was Choi [1]. A "nanofluid" is a liquid that contains ultrafine particles having a diameter of less than 50 nm, often metal or metal oxide. Applications for the combination of chemical reactions and heat and mass transfer issues may be found in many different sectors, and engineering domains, including nuclear power plants, gas turbines, various aircraft propulsion systems, missiles, satellites, spacecraft, biological domains, and medicinal procedures. At high operating temperatures, the radiation effect can be quite significant, making the effects of radiation on MHD flow and heat transfer problems more important in industries. (challenges related to the effects of radiation on MHD flow and heat transfer find its significance at high temperatures). Several features of mass transfer, heat transfer, and nanofluid flow with MHD radiation have been examined by several researchers. In their description of heat flow and transport, Wu as well as Zhao [2] laid forth the fundamentals of nanofluid use in engineering research. The impact of heat transmission on nanofluid flow and the consequences of double stratification on boundary layer flow in the context of a vertical plate was discussed by Ibrahim and Makinde [3]. The MHD alumina water nanofluid flow as well as mass transfer across a flat plate with certain slip conditions were examined by Singh and Kumar [4]. Sheikholeslami and Rokni [5] used the transverse magnetic field to investigate the review of MHD and heat transmission of nanofluid. The two-dimensional movement and heat transmission of Casson nanofluid across a cylinder or plate, as well as the effects of thermophoresis as well as Brownian motion phenomena, are examined by Farooq *et al*. [6]. Additionally, the impacts of bioconvection, exponential thermal sink/source, and motile microorganisms are taken into account. A numerical analysis of the MHD radiative motion of the near-stagnation point over an exponentially stretchable Cross nanofluid surface with a variable heat source/sink was addressed by Srinivasa Babu *et al*. [7].

Ramesh Babu et al. [8] have not paid much attention to unsteady MHD Non-Newtonian free convective flow through a porous media via a semi-infinite vertical permeable moving plate under the presence of radiation absorption. They researched the flow properties of the visco-elastic fluid and analyzed how radiation absorption is taken into account in the energy equation. A mixed convective magnetohydrodynamically responding two-dimensional non-Newtonian fluid via a vertical exponentially stretchable impermeable barrier was reported by Srinivasa Babu et al. [9] together with temperature and concentration distributions. The mixed convective MHD 2D Williamson fluid is numerically explored under suitable circumstances, including both masses and heat transport rates, via an exponentially

Cite as: A.D. Reddy, P.R.D. Reddy, B.L. Kuntumalla, S.L. Madhura, P. Areti, East Eur. J. Phys. 3, 236 (2024), https://doi.org/10.26565/2312-4334-2024-3-23

vertical stretching surface. The MHD boundary layer flow of an exponentially expanding sheet with a thermally stratified medium in the presence of suction was examined by Reddappa et al. [10]. The precise solutions for the propulsion of Ree-Eyring liquid under different effects, including Joule heating, MHD, and Hall currents, have been provided by Bhatti and Rashidi [11].

Newtonian fluids have a major part in many biological applications, flow processes in natural occurrences, and mechanical systems, which has led to a lengthy history of study in this area. Numerous models, including the Ellis, Carreau, Williamson, Jeffrey, Eyring-Powell, and Casson fluids, have been presented based on their rheological results. The Casson fluid model is among the models that people use the most often. Thick fruit juices, tomato catchup, and plasma are associated with Casson fluid. Red blood's characteristics match those of Casson fluid as well. When certain important components, such as protein, fibrinogen, and globulin, are present Human red blood cells (RBCs) can create connected formations called aggregates or rouleaux in plasma. The yield stress resulting from Rouleaux's plastic solid state is related to the fixed initial stress of Casson's fluid. The non-linear quantitative description of Casson's model has been used to formulate printing solutions [12], silicon solvents [13], and polymers [14]. Ali et al. [15] performed a computer investigation on the pulsatile pushing of Casson liquid in a porous channel using a finite difference method. Majeed et al. [16] investigate the effects of slip and MHD 2D bioconvection non-Newtonian Casson nanofluid flow towards a nonlinear stretchable surface in the presence of nanoparticles and motile gyrotactic microorganisms. The Optimal Homotopy Analysis Method (OHAM) has been used by Sohail et al. [17] to address the boundary layer Casson liquid flow on a linearly elongating surface. They examined the Casson fluid motion taking into account Joule heating, MHD, and stretching surface using the RK45 technique as outlined by Kumar and Srinivas [18], and Sreenivasulu et al. [19]. Kataria and Patel [20] have provided MATLAB simulations for the MHD Casson liquid propulsion past an oscillating vertical plate. A small number of further studies in the Casson fluid with effects from magnetic fields are presented. Along with others, RajuVenkateswara [21] In the presence of a chemical reaction, the effects of slip and produced magnetic field on a non-linear convective Casson fluid in a vertical past plate with an embedded porous medium are studied theoretically. The no-slip boundary requirements are flawed because fluid flow near a container's walls often differs from the surface velocity of the container. Because of this actual feature of the flow, many slip boundary conditions have been suggested by researchers. Thermal radiation is more common in engineering domains when temperatures are high, especially in tiny convective thermal transfer systems. Moreover, thermal radiation is crucial for regulating thermal transfer schemes and preserving the temperature throughout polymer synthesis operations. As a result, studies on the effects of radiation on fluid flow systems have begun. Mandal and Mukhopadhyay [22] have shown, for example, the thermal investigation of micropolar liquid past a stretching surface under the measurements of radiated environment impacts using a shot scheme. The free convective flow of a non-Newtonian fluid in a vertical deformable porous stratum with the influence of Darcy law was studied by Sreenadh et al. [23]. They noticed that both viscous and Darcy dissipations produce heat inside the fluid.

One may derive the blowing effect from Stefan\Prime's issue, and Stefan's blowing effects are practically significant in many scenarios. The effects of Stefan blowing on a movement involving the transfer of nanofluid on stretched plates were described by Fang and Jing [24]. They observed that the blowing improves the flow's velocity. The potential significance of Stefan blowing was noted by Hamid et al. [25], who also outlined the characteristics of Stefan blowing on species movement for stagnation point flow. The effect of Stefan blowing on the movement of Casson micro fluid due to a stretched part was examined by Lund et al. [26]. Mass conveys oscillated during the flow due to mass blowing at the partition. The effects of Stefan blowing over a bio-convective caused by a stretched cylinder were documented by Rana et al. [27]. Ellahi and his coauthors [28] were able to precisely solve critical flows when nonlinear slip was present in 2010. This issue also takes into account the more general slip condition at the border that Thompson and Troian [29] presented. The effects of the Thompson-Troian slip condition and Cattaneo-Christov heat flow across a stretched sheet were investigated by Ahmad and Nadeem [30]. The effects of a chemical reaction and Thompson and Troian slip on nanofluid flow via a stretching/shrinking sheet on a stagnation zone were described by Ramzan et al. [31]. The effects of the Riga surface and Thompson and Troian slip conditions on mixed convection nanofluid flow were covered by Nadeem et al. [32]. In conjunction with the first-order compound response, Dey et al. [33] recently examined the combined effects of Stefan blowing and Thompson and Troian slip on the forced convective motion of nano liquid across a nonabsorbent plate. They found that when the levels of the Stefan blowing parameter S increase, the skin friction coefficient decreases, and as the slip parameter δ and critical shear rate β rise, the mass transfer rate decreases. The precise nature of the link between these characteristics is not well understood. Further investigation is necessary in the field of existing research about the impact of the Thompson and Troian slip condition. There isn't a single published work that discusses the Stefan flow of nanofluid when uniform shear is present.

The purpose of this paper is to examine the effects of Thompson-Troian slip and Stefan blowing on the Casson nanofluid flow. In a uniform shear, we additionally take into account the impacts of radiation, chemical reactions, Joel heat, and MHD porous media. Appropriate transformations lead to a self-similar version of the leading equations. The R-K shooting technique is then used to solve these equations. When the produced findings and the available data are compared, they demonstrate perfect agreement. The impacts of several factors on the fields of hotness, nanoparticle concentration, velocity slope, and velocity are investigated. Visual representations are used to aid in comprehending these impacts.

2. FORMULATION OF THE PROBLEM

Consider a forced convection Casson micro-liquid flow across a fixed plate in the medium that has a very tiny width and a large span (see Fig. 1). The axis is normal relative to the axis's upward-directed plate. The magnetic field that is generated is assumed to be perpendicular to the plate. The transverse magnetic field's intensity is increased by the magnetic field. Considering that the velocity apparatuses are, respectively, running parallel and normal to the plate. Given the circumstances stated above, the rheological formulas are [33] provided by

$$\tau_{ij} = \begin{cases} 2\left(\mu_B + \frac{p_y}{\sqrt{2\pi}}\right)e_{ij,} & \pi > \pi_c, \\ 2\left(\mu_B + \frac{p_y}{\sqrt{2\pi_c}}\right)e_{ij,} & \pi < \pi_c, \end{cases}$$

in which, P_y is the Casson's yield stress, the scientific expression preordained for the yield stress possibly will be articulated as $P_y = \frac{\mu_B\sqrt{2\pi}}{\beta}$ where μ_B is the Casson fluid's lively viscosity, π signifies the product of the deformation rate's constituent finished themself $\left(\pi = e_{ij}\, e_{ij}\right)$, as well π_c symbolizes the critical value created on the Casson fluid model. In the occasion $\left(\pi > \pi_c\right)$ of Casson fluid motion, the aforementioned is feasible in the case of $\mu = \mu_B + \frac{P_y}{\sqrt{2\pi}}$, By supernumerary, the Casson fluid viscosity remains now (which depends on) contingent on the Casson parameter β, in addition dynamic viscosity μ_B, and it (delete) can be inscribed as: $\mu = \mu_B\left(1 + \frac{1}{\beta}\right)$

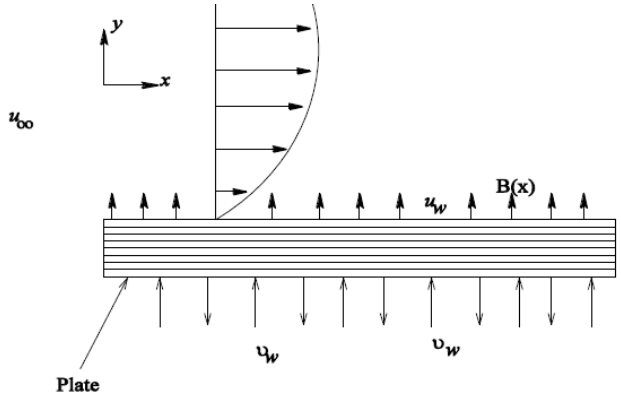

Figure 1. Sketch of the physical flow problem

$$\frac{\partial u}{\partial x} + \frac{\partial v}{\partial y} = 0 \tag{1}$$

$$u\frac{\partial u}{\partial x} + v\frac{\partial u}{\partial y} = \upsilon_f\left(1 + \frac{1}{\beta}\right)\frac{\partial^2 u}{\partial y^2} - \frac{\sigma B_0^2}{\rho_f}(u - u_\infty) - \frac{\mu}{k}u \tag{2}$$

$$u\frac{\partial T}{\partial x} + v\frac{\partial T}{\partial y} = \alpha\frac{\partial^2 T}{\partial y^2} + \frac{(\rho c)_p}{(\rho c)_f}\left[D_B\frac{\partial C}{\partial y}\frac{\partial T}{\partial y} + \frac{D_T}{T_\infty}\left(\frac{\partial T}{\partial y}\right)^2\right] - \frac{1}{(\rho c)_f}\frac{\partial q_r}{\partial y} + \frac{\nu}{(\rho c)_f}\left(1 + \frac{1}{\beta}\right)\left(\frac{\partial u}{\partial y}\right)^2 \tag{3}$$

$$u\frac{\partial C}{\partial x} + v\frac{\partial c}{\partial y} = D_B\frac{\partial^2 C}{\partial y^2} + \frac{D_T}{T_\infty}\frac{\partial^2 T}{\partial y^2} + k_1\left(C - C_\infty\right) \tag{4}$$

Here,*u*and*υ* is the Casson fluid parameter, indicates the uniform magnetic field, denotes the electrical conductivity, k is the permeability parameter, corresponds to the fluid's specific heat, t is the time, k denotes the thermal conductivity, denotes the radiative heat flux, and are the parts of the velocity in the x and y directions, respectively. The temperature along the free stream is T, and so are the two temperatures. The variables denoted by α are the thermal diffusivity, free stream velocity, effective heat capacity of the nanofluid as well as nanoparticles, as well as Brownian and thermophoretic diffusion coefficients, correspondingly. C represents the volume percentage of nanoparticles, is the free stream focused attention, $k_1 = \frac{k_0}{x^{2/3}}$, ($k_0$ being constant) is the rate of chemical reaction, wherever $k_1 > 0$ and $k_1 < 0$ indicates that there are chemical processes that are both productive and detrimental. There are several scenarios where the response rate may change inversely with distance. Reaction rate has thus been taken (as a) significant variable in this text. The following list contains the suitable boundary circumstances regarding the present problem,

$$u=\gamma\left(1-\zeta\frac{\partial u}{\partial y}\right)^{-1/2}\frac{\partial u}{\partial y},\ v=\frac{-D_B}{\left(1-C_w\right)}\frac{\partial C}{\partial y},\ T=T_\infty,\ C=C_w \text{ at } y=0 \tag{5a}$$

$$u=u_\infty\left(y\right)=\beta_1 y,\ T=T_\infty,\ C=C_\infty \text{ at } y\to\infty \tag{5b}$$

Here, $\gamma=\gamma_0 x^{1/3}$ is the Navier slip length, γ_0 is the slip factor, ζ is the reciprocal of the shear rate and $\beta_1=v/L^2$ remains constant. In this case, the consistency of The idea of conservation of mass is shown in Equation (1). Equation (2) describes the momentum equation using boundary layer estimations, and it may be applied to any case involving incompressible fluid flow. The left-hand side (l.h.s) of the text represents the inertial phrases that are discussed in each article. Conversely, the first term on the right (r.h.s.) represents the viscosity term, magnetic field, and overall porous media properties found in all of the studies listed in the text. The initial term in the r.h.s. of Eqs. (3) and (4) transmit a diffusive component, while the l.h.s. of those equations indicate the convective term to earn mass transfer and heat transport, respectively. The last two variables in (3)'s r.h.s. stand for the effects of radiation, Brownian motion, thermophoresis, velocity distribution, and Joel heat – all of which have been found in earlier research [12,20,27]. First-order chemical processes are represented by the last item on the r.h.s. of (4) and have been examined by Daniel et al. [12,23], Dey, and Mukhopadhyay [27]. The thermophoresis effect is shown by the second term on r.h.s. of (4) and is seen in [12,20,27]. (5a) has two boundary conditions: [29–30] provides the second boundary condition for Stefan blowing, while [30–33] provides the first boundary condition for slip. One can locate the uniform shear flow in [36–38] that results in the first condition of (5b). In addition to the mass transfer problem over a flat plate, (5b) provides additional free-stream conditions for every flow and heat.

Resemblance examination in addition to the explanation process

The subsequent similarity conversion relations remain now placed for u,v as

$$u=\frac{\partial\psi}{\partial y},v=-\frac{\partial\psi}{\partial x} \tag{6}$$

Anywhere, ψ is the stream function. Over, let us familiarize the subsequent dimensionless variables,

$$\eta=\frac{y}{L}\left(\frac{x}{L}\right)^{-1/2},\ \psi=v\left(\frac{x}{L}\right)^{2/3}f\left(\eta\right)\text{and}\,\theta=\frac{T-T_\infty}{T_w-T_\infty},\ \phi=\frac{C-C_\infty}{C_w-C_\infty} \tag{7}$$

The enlargement of native thermal energy is

$$-\frac{\partial q_r}{\partial y'}=4\ \alpha\ \sigma\ (T_\infty'^4-T'^4) \tag{8}$$

where σ and α are Stefan-Boltzmann constant in addition to the absorption coefficient. Decrease the Eq. (3) through using Eq. (8) we get

Using the relatives (6)–(7) in the border layer Eq. (2), vigor Eq. (3) in addition to attentiveness Eq. (4) the subsequent equations remaingot.

$$\left(1+\frac{1}{\beta}\right)f'''+\frac{2}{3}f\,f''-\frac{1}{3}\left(f'\right)^2-\left(M+\frac{1}{K}\right)f'=0 \tag{9}$$

$$\frac{1}{\mathrm{Pr}}\left(1+\frac{4R}{3}\right)\theta''+N_b\,\theta'\phi'+N_t\left(\theta'\right)^2+\frac{2}{3}f\,\theta'+Ec\left[\left(f'\right)^2+\left(f''\right)^2\right]=0 \tag{10}$$

$$\phi''+\frac{N_t}{N_b}\theta''+Le\left[\frac{2}{3}f\,\phi'-k\phi\right]=0 \tag{11}$$

wherever $M=\sqrt{\frac{x\,\sigma}{LU}}\,\mathrm{B}_0$ is the Magnetic parameter, $K=\frac{\mu}{x^{2/3}Lk}$ is the Porous medium parameter, $\mathrm{Pr}=\frac{v}{\alpha}$ is the Prandtl number, R is the radiation $Le=\frac{v}{D_B}$ is the Lewis number, $N_b=\frac{\left(\rho c\right)_p D_B\left(C_w-C_\infty\right)}{\left(\rho c\right)_f v}$ is the Brownian motion parameter and $N_t=\frac{\left(\rho c\right)_p D_T\left(T_w-T_\infty\right)}{\left(\rho c\right)_f v T_\infty}$ is the thermophoresis parameter, $k=k_1x^{2/3}$ is the rate at which chemicals react parameter; it shows both constructive as well as destructive chemical processes, but it also shows the absence of chemical reactions. In light of this, boundary requirements ultimately turn into

$$f=\frac{3S}{2Le}\phi',\ f'=\delta\left(1-\beta_1 f''\right),\ \theta=1,\ \phi=1 \text{ at } \eta=0 \tag{12a}$$

$$f''=1,\ \theta=0,\ \phi=0 \text{ at } \eta\to\infty \tag{12b}$$

where $\delta=\gamma\frac{1}{L}\left(\frac{x}{L}\right)^{-1/3}=\gamma_0\frac{1}{L^{2/3}}$, is the velocity slip parameter and $\beta_1=\zeta\frac{v}{L^2}$, is the critical shear rate. $S=\frac{\left(C_w-C_\infty\right)}{1-C_w}$ is the Stefan blowing parameter. $S>0$ shows mass movement from fluid to plate (mass suction), but shows mass transfer from plate to fluid (mass blowing) [13,15].

2.2. Physical quantities

Sherwood number, Nusselt number, as well as skin friction coefficient, are the non-dimensional numbers of practical relevance Sh_x, Nu_x, C_f are given:

$$C_f=\frac{\tau_w}{\rho L^2}, \text{ where } \tau_w=\mu\left(1+\frac{1}{\beta}\right)\left(\frac{\partial u}{\partial y}\right)_{y=0},\ Nu_x=\frac{xq_w}{k\left(T_w-T_\infty\right)}, \text{ and } Sh_x=\frac{xq_m}{D_B\left(C_w-C_\infty\right)}$$

Anywhere q_w, q_m suggests the mass and heat fluxes, besides specifying the thermal conductivity of the nanofluid.

$$q_w=\left[-\left(k+\frac{16\sigma^*T_\infty^3}{3k^*}\right)\left(\frac{\partial T}{\partial y}\right)\right]_{y=0},\ q_m=-D_m\left(\frac{\partial C}{\partial y}\right)_{y=0}$$

Replacing q_w, and q_m in the above equations, we get.

$$\mathrm{Re}_x^{1/2}\,C_f\sqrt{\frac{\upsilon x}{L}}=\left(1+\frac{1}{\beta}\right)f''(0),\ \mathrm{Re}_x^{1/2}\,Nu_x\sqrt{\frac{\upsilon x}{L}}=-\left(1+\frac{4}{3}R\right)\theta'(0),\ \mathrm{Re}_x^{1/2}\,Sh_x\sqrt{\frac{\upsilon x}{L}}=-\phi'(0).$$

where $\mathrm{Re}_x^{-1/2}=\frac{U_w}{\upsilon}$ is the local Reynolds number.

3. RESULTS AND DISCUSSION

3.1.Validation of results:

The present findings (for the no-slip border situation in the absence of Stefan blowing) are contrasted with the available published results of Blasius [34], Ishak et al. [35], Verma et al. [36], and Dey et al. [30] to verify the accuracy of the applied numerical scheme. Table 2 highlights an ideal convention alongside the available results.

3.2. Analysis of results

Numerical computations have been performed using the method outlined in the preceding section for various values of dissimilar parameters to provide a clear picture of the current issue. Figures 2 through 34 provide numerical data that illustrate the results.

The effects of the Casson fluid parameter on the profiles of temperature, concentration, and velocity are shown in Figs. 2, 9, and 22. When the critical shear rate and velocity slip parameter are present, the temperature rises while concentration and velocity drop. The effects of the magnetic parameter on the profiles of velocity, temperature, and concentration are shown in Figs. 3, 15, 23, and 4. As velocity and concentration increase, temperature exhibits the opposite behaviors in the presence of the critical shear rate and velocity slip parameter. Figures 4, 16, and 34 illustrate how the Porous medium parameter affects the profiles of temperature, concentration, and velocity. As the parameter increases, so do the profiles of concentration and velocity; however, when the critical shear rate and velocity slip parameters are present, the temperature exhibits the opposite behavior. The effects of critical shear rate parameters on temperature, concentration, and velocity profiles are depicted in Figs. 5, 18, and 29. Increasing the critical shear rate parameter causes an increase in concentration and velocity, while the presence of the Stefan blowing parameter causes the temperature profile to exhibit the opposite behaviors. The temperature drops for various velocity Thompson-Troian slip parameter values in Figures 6 and 21, respectively, although concentration oscillates in the presence of in Figure 28. The Lewis number's effects on velocity, temperature, and concentration profiles are shown in Figs. 7, 19, and 26. As, temperature and velocity dropped, the concentration profile displayed the opposite behaviors when the Stefan blowing parameter was present. Figure 8 illustrates the reduction in velocity, whereas Figure 20 displays a rise in temperature for varying values of the Stefan blowing parameter. However, Figure 30 displays concentration oscillations when certain values are present. For increasing values, the temperature results are shown in Figs. 12, 13, and 14 together with the impacts of the Brownian motion parameter, the thermophoresis parameter, and the Eckert number. For the values of, there is a temperature rise. The concentration findings with the impacts of the Eckert number, Thermophoresis parameter, and Brownian motion parameter are shown in Figs. 24, 25, and 33. As the concentration profile increases, it oscillates in the presence of. The findings of temperature in relation to the radiation parameter and Prandtl number are shown in Fig. 10, and 11. As and increases,

the fluid's temperature fluctuates in their presence. In the presence of, the concentration profiles from Figs. 31 and 32 show the same performance. We can see from Figures 17 and 27 that, in the presence of, the temperature and concentration are falling as the chemical reaction parameter increases.

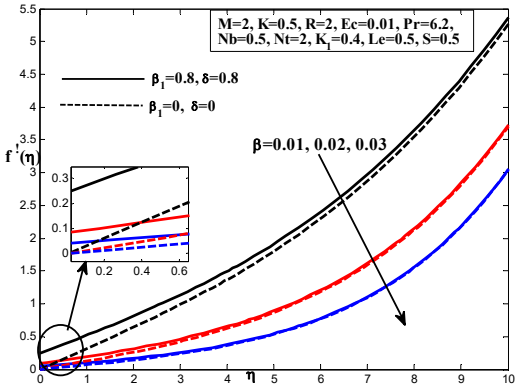

Figure 2. Velocity outline for different values of β

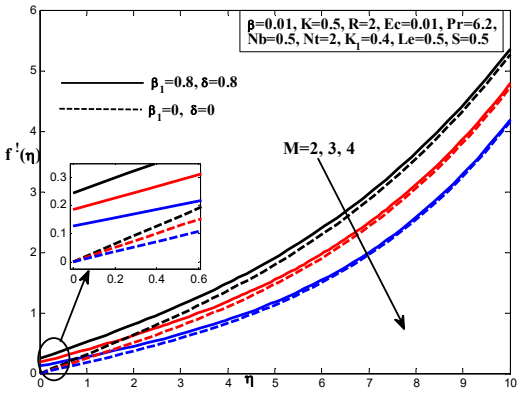

Figure 3. Velocity outline for different values of M

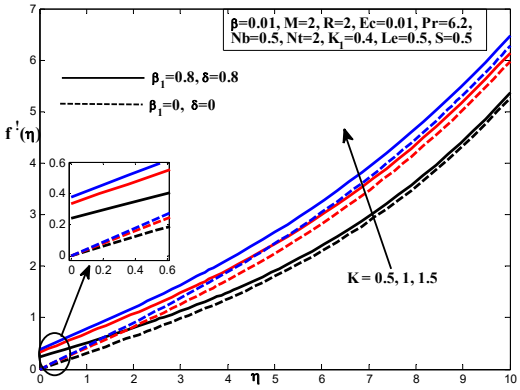

Figure 4. Velocity outline for different values of K

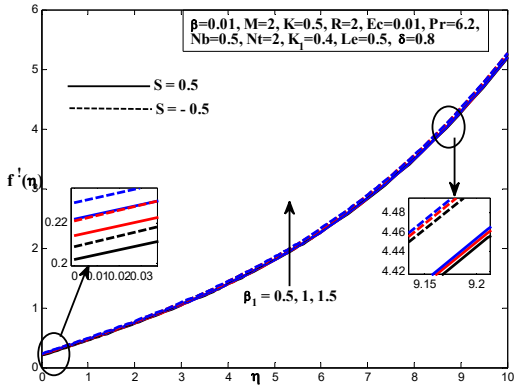

Figure 5. Velocity outline for different values of β_1

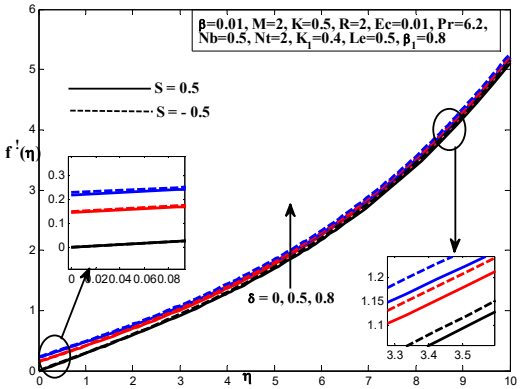

Figure 6. Velocity outline for different values of δ

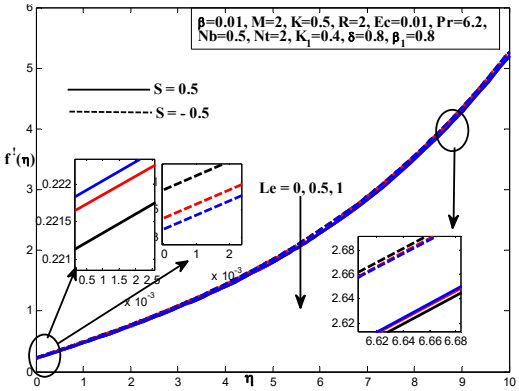

Figure 7. Velocity outline for different values of Le

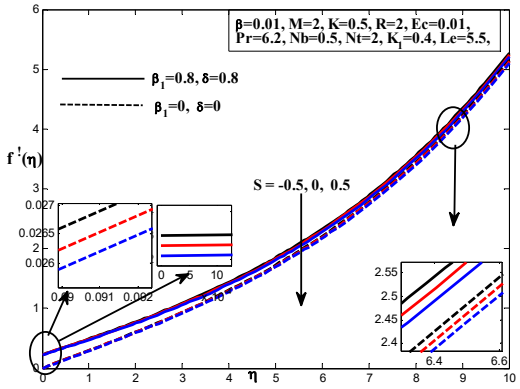

Figure 8. Velocity outline for different values of S

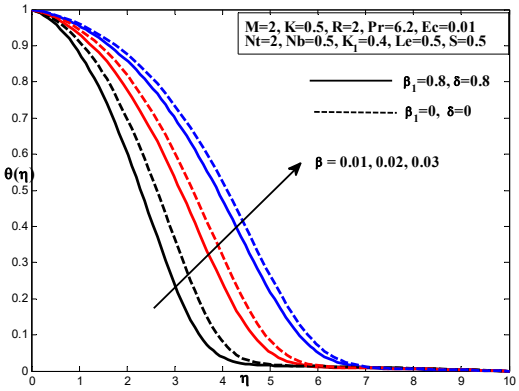

Figure 9. Temperature outline for various values of β

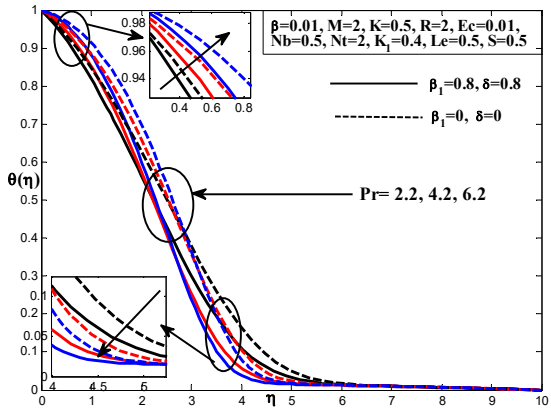

Figure 10. Temperature outline for various values of Pr

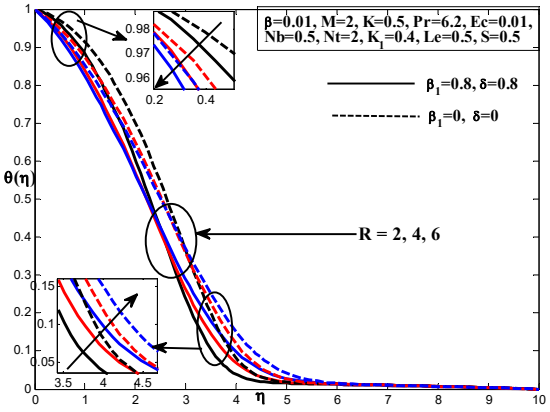

Figure 11. Temperature outline for various values of R

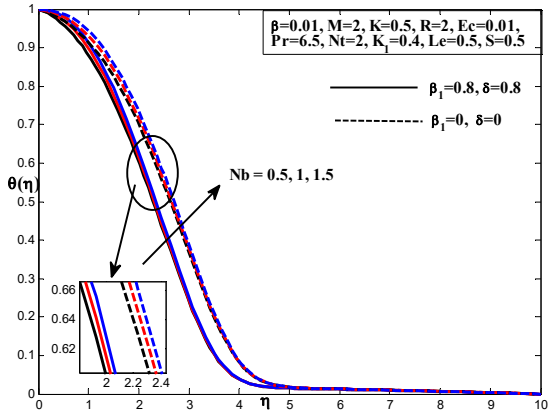

Figure 12. Temperature outline for various values of N_b

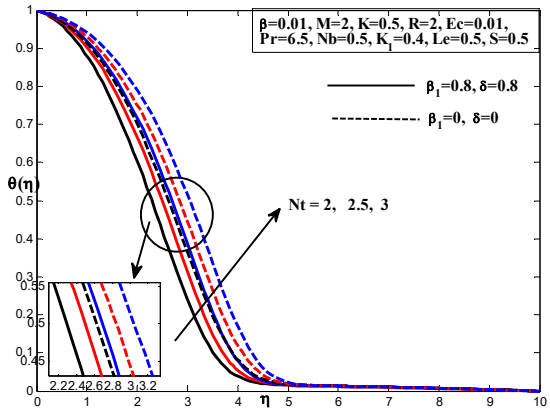

Figure 13. Temperature outline for various values of N_t

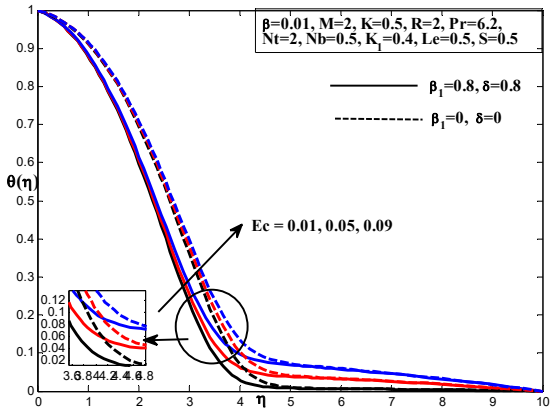

Figure 14. Temperature outline for various values of Ec

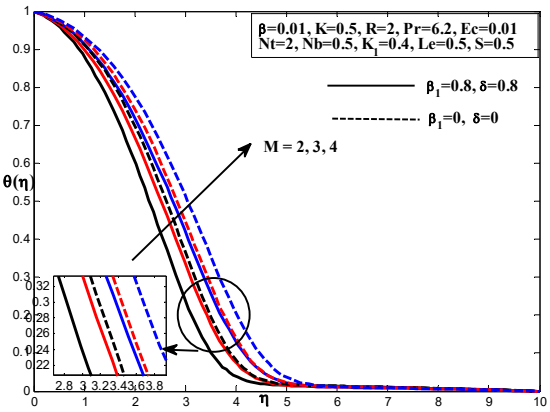

Figure 15. Temperature outline for various values of M

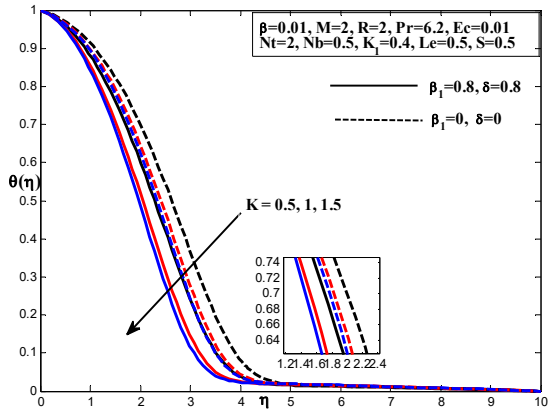

Figure 16. Temperature outline for various values of K

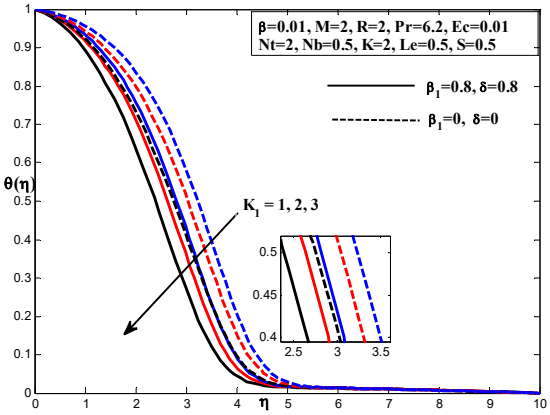

Figure 17. Temperature outline for various values of K_1

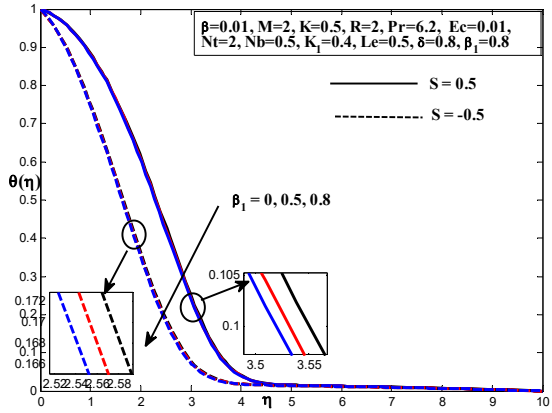

Figure 18. Temperature outline for various values of β_1

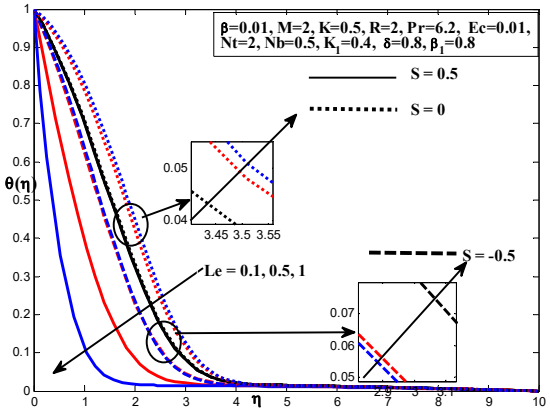

Figure 19. Temperature outline for various values of Le

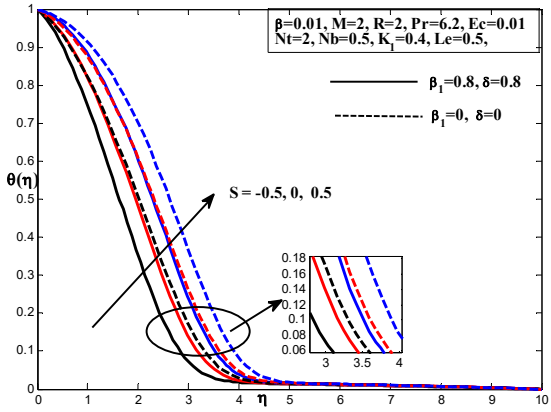

Figure 20. Temperature outline for various values of S

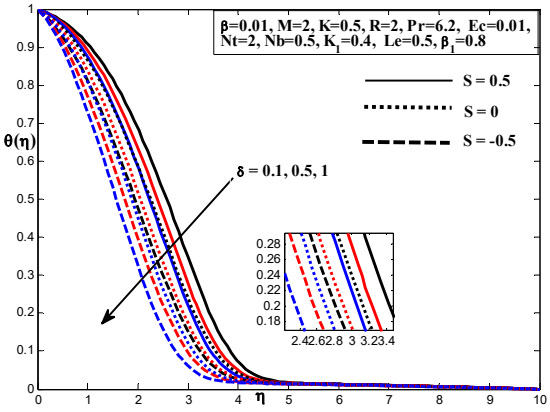

Figure 21. Temperature outline for various values of δ

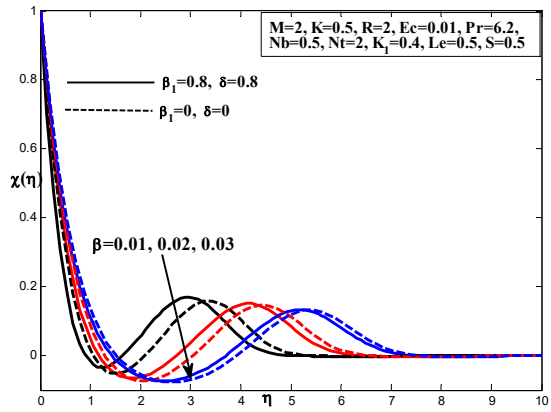

Figure 22. Concentration outline for various values of β

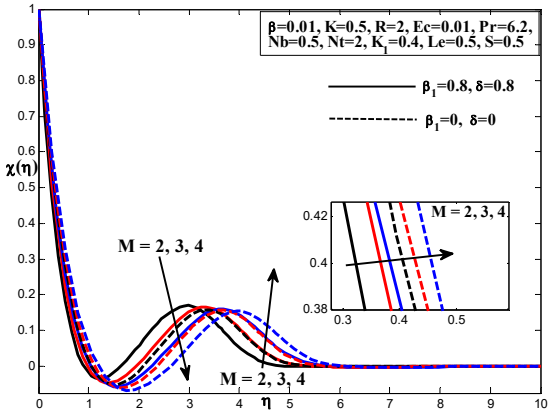

Figure 23. Concentration outline for various values of M

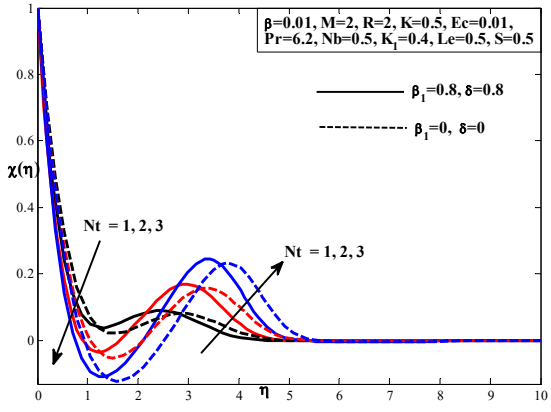

Figure 24. Concentration outline for various values of N_t

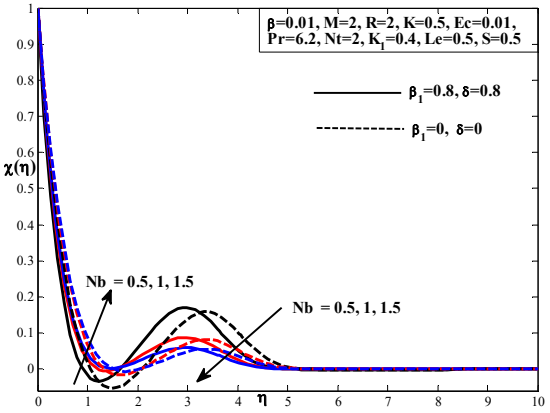

Figure 25. Concentration profile for various values of N_b

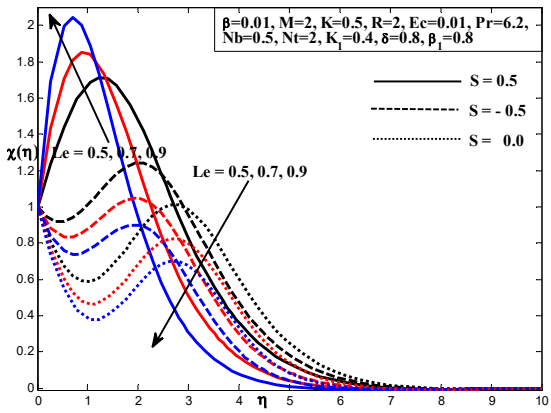

Figure 26. Concentration profile for various values of Le

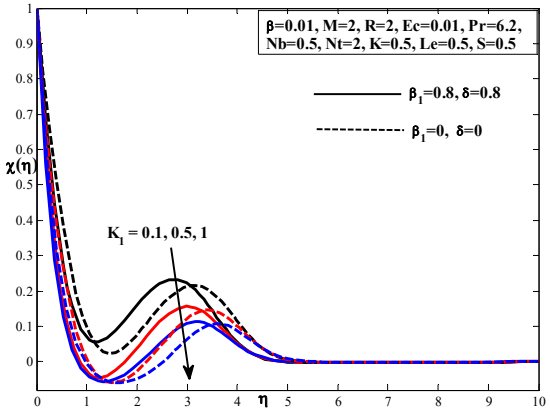

Figure 27. Concentration profile for various values of K_1

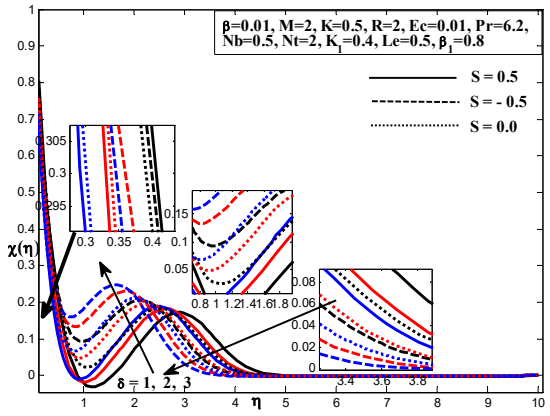

Figure 28. Concentration profile for various values of δ

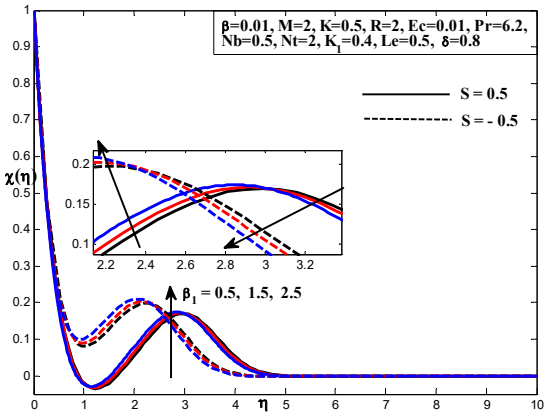

Figure 29. Concentration profile for various values of β_1

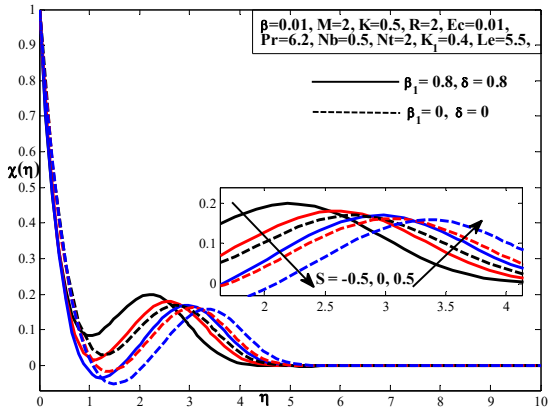

Figure 30. Concentration profile for various values of S

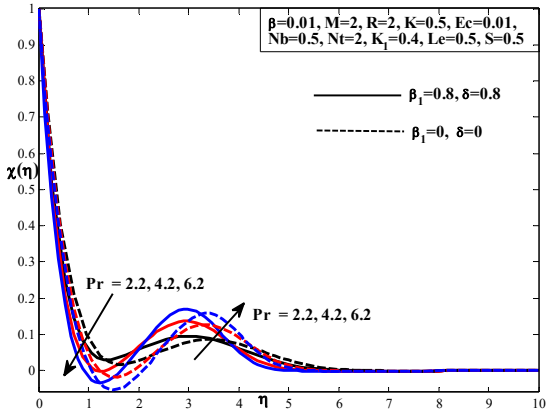

Figure 31. Concentration profile for various values of Pr

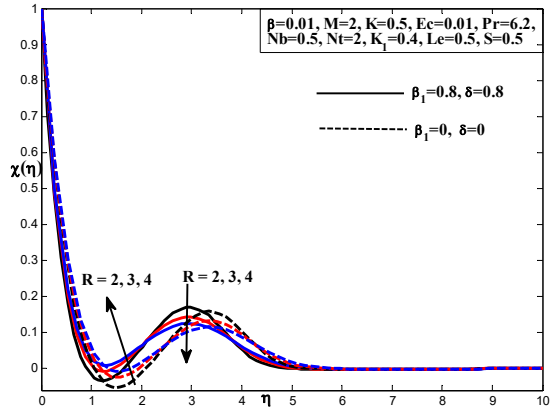

Figure 32. Concentration profile for various values of R

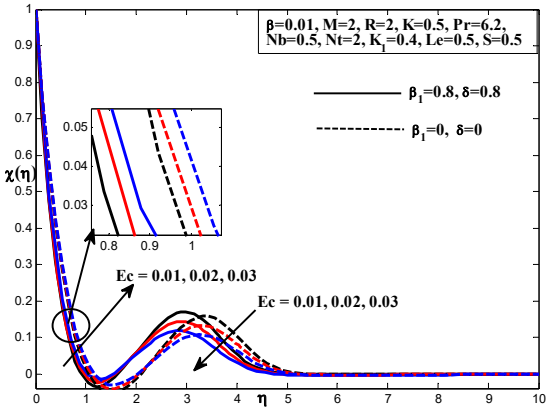

Figure 33. Concentration profile for various values of Ec

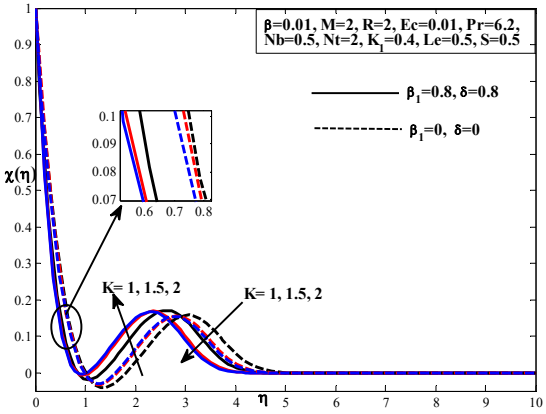

Figure 34. Concentration profile for various values of K

Table 1 displays skin friction, Nusselt number, and shear wood number, which are consistent with earlier research. The skin friction coefficient decreases when development occurs, whereas the parameters show the opposite trend (Table 2). When the parameters are included, the Nusselt number rises, and when the parameters are excluded, the Nusselt number decreases (Table 2). For the parameters, the opposite result is seen when the mass transfer rate decreases. Pr, Ec (Table 2).

Table 1. Values of $f''(0)$, $-\theta'(0)$, $-\phi'(0)$ for $N_t = \beta_1 = \delta = S = 0$ and non-dimensional parameters.

β	M	Pr	R	Ec	K	N_t	K_1	β_1	δ	S	$f''(0)$	$-\theta'(0)$	$-\phi'(0)$
0	0	0	0	0	0	0	0	0	0	0	0.759875	0.0615431	1.4957
								0.1			0.759775	0.0699181	1.53978
								0.2			0.753338	0.0779771	1.58098
								0.3			0.741848	0.0855734	1.61892
									0.1		0.740226	0.0864321	1.62315
									0.2		0.738348	0.087386	1.62785
									0.3		0.736152	0.0884532	1.63309
						0.1					0.752703	0.159365	1.50014
						0.2					0.743802	0.117561	1.57161
						0.3					0.729837	0.0679804	1.6839
										0.1	0.717368	0.0620508	1.78433
										0.2	0.7057	0.0570051	1.87847
										0.3	0.694696	0.052655	1.9674
0.01											1.256512	0.1547812	1.254874
0.02											1.325413	0.1454217	1.225487
	1										0.785213	1.2154784	1.254784
	2										0.795846	1.3524781	1.226487
		2.2									0.759875	1.2345478	0.984577
		4.2									0.745412	1.2254784	0.995841
			2								0.859875	1.5414784	1.024578
			4								0.959875	1.6457841	0.985689
				0.01							0.689875	0.2514782	1.02548
				0.02							0.659875	0.3215478	1.032659
					0.5						0.541741	0.2154784	1.312154
					1						0.442156	0.2165478	1.301215

Table 2. $f'(0)$ for flow over a plate when $\delta = 0 = \beta =$ S = k.

Verma et al. [33] $\lambda = e = \delta = s = K = 0$	Ishak et al. [32] $\lambda = 0$	Blasius [31]	Dey et al. [30]	Present work $\beta = M = R = K = 0$
0.33206	0.3321	0.332	0.332566	0.3321265

4. CONCLUDING REMARKS

The flow of a Stefan-Cassonnanofluid across a plate has been studied considering radiation, magnetohydrodynamics (MHD), shear flow, and porous material. The consequences of the Thompson-Troian slide at

the border were also investigated. When the research compared the numerical answers to the existing data, it discovered a very good match. The findings led to the following observations being made.

(i) As the thermophoresis parameter values increase and decrease, the temperature rises. For increasing values of the Brownian motion parameter, concentration is seen.

(ii) As the chemical reaction values rise, the temperature drops and the concentration fluctuates parameter (k).

(iii) The liquid absorbs heat from the plate.

(iv) The skin friction coefficient decreases as the Stefan blowing parameter S increases.

(v) As slip parameter δ and critical shear rate β increase, the mass transfer rate decreases.

ORCID

Parandhama Areti, https://orcid.org/0000-0002-7242-895X

REFERENCES

[1] S.U.S. Choi, "Enhancing thermal conductivity of fluids with nanoparticles," in: *Developments and Applications of Non-Newtonian Flows*, edited by D.A. Siginer, and H.P. Wang, (ASME, New York, 1995), pp. 99–105.

[2] J.M. Wu, and J. Zhao, "A review of nanofluid heat transfer and critical heat flux enhancement research gap to engineering application," Progr. Nuclear Energy, **66**, 13–24 (2013). https://doi.org/10.1016/j.pnucene.2013.03.009

[3] W. Ibrahim, and O.D. Makinde, The effect of double stratification on boundary-layer flow and heat transfer of nanofluid over a vertical plate, Comput. Fluids, **86**, 433–441 (2013). https://doi.org/10.1016/j.compfluid.2013.07.029

[4] P. Singh, and M. Kumar, Mass transfer in MHD flow of alumina water nanofluid over a flat plate under slip conditions, Alex. Eng. J. **54**, 383–387 (2015). https://doi.org/10.1016/j.aej.2015.04.005

[5] M. Sheikholeslami, and H.B. Rokni, Simulation of nanofluid heat transfer in the presence of magnetic field: a review, Int. J. Heat Mass Transf. **115**, 1203–1233 (2017). https://doi.org/10.1016/j.ijheatmasstransfer.2017.08.108

[6] U. Farooq, H. Waqas, S.E. Alhazmi, A. Alhushaybari, M. Imran, R. Sadat, T. Muhammad, *et al*., "Numerical treatment of CassonnanofluidBio convectional flow with heat transfer due to stretching cylinder/plate: Variable physical properties," Arabian Journal of Chemistry, **16**(4), (2023). https://doi.org/10.1016/j.arabjc.2023.104589

[7] K.S.S. Babu, A. Parandhama, and R.B. Vijaya, "Significance of heat source/sink on the radiative flow of Cross nanofluid across an exponentially stretching surface towards a stagnation point with chemical reaction," Heat Transfer, **51**(4), 2885–2904 (2021). https://doi.org/10.1002/htj.22428

[8] K.R. Babu, A. Parandhama, K.V. Raju, M.C. Raju, and P.V.S. Narayana, "Unsteady MHD Free Convective Flow of a Visco-Elastic Fluid Past an Infinite Vertical Porous Moving Plate with Variable Temperature and Concentration," Int. J. Appl. Comput. Math. **3**, 3411–3431 (2017). https://doi.org/10.1007/s40819-017-0306-8

[9] K.S.S. Babu, A. Parandhama, and R.B. Vijaya, "A Numerical Investigation of chemically reacting 2D Williamson fluid over a vertical exponentially stretching surface," South East Asian J. of Mathematics and Mathematical Sciences, **16**(3), 295-310 (2020).

[10] B. Reddappa, A. Parandhama, K. Venkateswara Raju, and S. Sreenadh, "Analysis of the Boundary Layer Flow of Thermally Conducting Jeffrey Fluid over a Stratified Exponentially Stretching Sheet," Turkish Journal of Computer and Mathematics Education, **12**(13), 730-739 (2021). https://doi.org/10.17762/turcomat.v12i13.8469

[11] M.M. Bhatti, and M.M. Rashidi, "Study of heat and mass transfer with Joule heating on magnetohydrodynamic (MHD) peristaltic blood flow under the influence of Hall effect," Propulsion and Power Research, **6**(3), 177-185 (2017). https://doi.org/10.1016/j.jppr.2017.07.006

[12] N. Casson, and C.C. Mill, *Rheology of Dispersed System*, vol. 84, (Pergamon Press, Oxford, 1959).

[13] W.P. Walwander, T.Y. Chen, and D.F. Cala, "Biorheology, An approximate Casson fluid model for tube flow of blood," Biorheology, **12**, 111-119 (1975). https://doi.org/10.3233/BIR-1975-12202

[14] G.V. Vinogradov, and A.Y. Malkin, *Rheology of Polymers*, (Mir Publisher, Moscow, 1979). (in Russian)

[15] A. Ali, H. Farooq, Z. Abbas, Z. Bukhari, and A. Fatima, "Impact of Lorentz force on the pulsatile flow of a non-Newtonian Casson fluid in a constricted channel using Darcy's law: a numerical study," Sci. Rep. **10**(1), 10629 (2020). https://doi.org/10.1038/s41598-020-67685-0

[16] A. Majeed, N. Golsanami, B. Gong, Q.A. Ahmad, S. Rifaqat, A. Zeeshan, and F.M. Noori, "Analysis of thermal radiation in magnetohydrodynamic motile gyrotactic micro-organisms flow comprising tiny nanoparticle towards a nonlinear surface with velocity slip," Alexandria Engineering Journal, **66**, 543–553 (2023). https://doi.org/10.1016/j.aej.2022.11.012

[17] M. Sohail, Z. Shah, A. Tassaddiq, P. Kumam, and P. Roy, "Entropy generation in MHD Casson fluid flow with variable heat conductance and thermal conductivity over a non-linear bi-directional stretching surface," Sci. Rep. **10**(1), 12530 (2020). https://doi.org/10.1038/s41598-020-69411-2

[18] C.K. Kumar, and S. Srinivas, "Influence of Joule heating and thermal radiation on unsteady hydromagnetic flow of chemically reacting Casson fluid over an inclined porous stretching sheet," Spec. Top Rev. Porous Media Int. J. **10**(4), 385-400 (2019). https://doi.org/10.1615/SpecialTopicsRevPorousMedia.2019026908

[19] P. Sreenivasulu, T. Poornima, and N.B. Reddy, "Influence of Joule heating and non-linear radiation on MHD 3D dissipating flow of Casson nanofluid past a non-linear stretching sheet," Nonlinear Eng. **8**(1), 661-672 (2019). https://doi.org/10.1515/nleng-2017-0143

[20] H. Kataria, and H. Patel, "Heat and mass transfer in magnetohydrodynamic (MHD) Casson fluid flow past over an oscillating vertical plate embedded in porous medium with ramped wall temperature," Propulsion and Power Research, **7**(3), 257-267 (2018). https://doi.org/10.1016/j.jppr.2018.07.003

[21] K.V. Raju, A. Parandhama, and M. Changalraju, "Induced Magnetic Field And Slip Effects on Non-Linear Convective Casson Fluid Flow Past a Porous Plate Embedded in Porous Medium," Journal of Xidian University, **14**(5), 1334-1343 (2020). http://dx.doi.org/10.37896/jxu14.5/148

[22] I.C. Mandal, and S. Mukhopadhyay, "Nonlinear convection in micropolar fluid flow past an exponentially stretching sheet in an exponentially moving stream with thermal radiation," Mech. Adv. Mater. Struct. **26**(24), 2040-2046 (2019). https://doi.org/10.1080/15376494.2018.1472325
[23] S. Sreenadh, M.M. Rashidi, K.K.S. Naidu, and A. Parandhama, "Free Convection Flow of a Jeffrey Fluid through a Vertical Deformable Porous Stratum," Journal of Applied Fluid Mechanics, **9**(5), 2391-2401 (2016). https://doi.org/10.18869/acadpub.jafm.68.236.25549
[24] T. Fang, and W. Jing, "Flow heat and species transfer over a stretching plate considering coupled Stefan blowing effects from species transfer," Commun. Nonlinear Sci. Numer. Simul. **19**, 3086–3097 (2014). https://doi.org/10.1016/j. cnsns.2014.02.009
[25] R.A. Hamid, R. Nazar, and I. Pop, "Stagnation point flow, heat transfer, and species transfer over a shrinking sheet with coupled Stefan blowing effects from species transfer," AIP Conf. Proc. **1784**, 050005 (2016), https://doi.org/10.1063/1.4966824
[26] L.A. Lund, Z. Omar, J. Raza, I. Khan, and E.S.M. Sherif, "Effects of Stefan blowing and slip conditions on unsteady MHD Casson nanofluid flow over an unsteady shrinking sheet: dual solutions," Symmetry, **12**(3) 487 (2020). https://doi.org/10.3390/sym12030487
[27] P. Rana, V. Makkar, and G. Gupta, "Finite element study of bio-convective Stefan blowing Ag-MgO/water hybrid nanofluid induced by stretching cylinder utilizing non-Fourier and Non-Fick's Laws," Nanomaterials, **11**, 1735 (2021). https://doi.org/10.3390/nano11071735
[28] R. Ellahi, T. Hayat, F.M. Mahomed, and A. Zeeshan, "Fundamental flows with nonlinear slip conditions: exact solutions," Z. Angew. Math. Phys. **61**, 877–888 (2010). https://doi.org/10.1007/s00033-010-0079-y
[29] P.A. Thompson, and S.M. Troian, "A general boundary condition for liquid flow at solid surfaces," Nature, **389**, 360–362 (1997). https://doi.org/10.1038/38686
[30] S. Ahmad, and S. Nadeem, "Flow analysis by Cattaneo–Christov heat flux in the presence of Thompson and Troian slip condition," Appl. Nanosci. **10**, 4673–4687 (2020). https://doi.org/10.1007/s13204-020-01267-4
[31] M. Ramzan, J.D. Chung, S. Kadry, Y.M. Chu, and M. Akhtar, "Nanofluid flow containing carbon nanotubes with quartic autocatalytic chemical reaction and Thompson and Troian slip at the boundary," Scient. Rep. **10**, 18710 (2020). https://doi.org/10.1038/s41598-020-74855-7
[32] S. Nadeem, S. Ahmad, and M.N. Khan, "Mixed convection flow of hybrid nanoparticle along a Riga surface with Thompson and Troian slip condition," J. Thermal Anal. Calorim. **143**, 2099–2109 (2020). https://doi.org/10.1007/s10973-020-09747-z
[33] S. Dey, S. Mukhopadhyay, and M. Begum, "Stefan flow of nanofluid and heat transport over a plate in company of Thompson and Troian slip and uniform shear flow," Forces in Mechanics, **9**, 100129 (2022). https://doi.org/10.1016/j.finmec.2022.100129
[34] H. Blasius, "Grenzschichten in FlussigkeitenmitkleinerReibung," Z. Math. Phys. **56**, 1–37 (1908).
[35] A. Ishak, R. Nazar, and I. Pop, "Flow and heat transfer characteristics on a moving flat plate in a parallel stream with constant surface heat flux," Heat Mass Transf. **45**, 563–567 (2009). https://doi.org/10.1007/s00231-008-0462-9
[36] A.K. Verma, A.K. Gautam, K. Bhattacharyya, A. Banerjee, and A.J. Chamkha, "Boundary layer flow of non-Newtonian Eyring–Powell nanofluid over a moving flat plate in Darcy porous medium with a parallel free-stream: Multiple solutions and stability analysis," Pramana J. Phys. **173**, 95 (2021). https://doi.org/10.1007/s12043-021-02215-9

ПОВНИЙ МГД ПОТІК СТЕФАНА НАНОРІДИНИ КАСОНА У ПОРИСТОМУ СЕРЕДОВИЩІ ЗА НАЯВНОСТІ ХІМІЧНОЇ РЕАКЦІЇ З ЕФЕКТОМ ТОМПСОНА, А ТАКОЖ ТРОЙАН-КОВЗАННЯ ПО ПЛАСТИНІ ЗА НАЯВНОСТІ ВИПРОМІНЮВАННЯ

Аніта Діві Редді[a], Прабхакара Редді Діві Редді[a], Бхаг'я Лакшмі Кунтумалла[b], Снеха Латха Мадхура[c,d], Парандхама Ареті[e]
[a]Департамент математики та комп'ютерних навичок, Центр підготовчого навчання, Університет технології та прикладних наук, Нізва, Султанат Оман – 611
[b]Факультет математики, Технічний кампус CMR, Медчал, Хайдерабад, Телангана-501401, Індія
[c]Департамент математики Академії менеджменту Самбхрам, Бангалор-560097, Індія
[d]Університет Самбхрам, Джизак, Узбекистан-130100
[e]Кафедра математики, Інститут аеронавігаційної техніки, Хайдарабад, Телангана-500043, Індія

У цій роботі ми повідомляємо про вплив ефекта Томпсона, ковзання Трояна та Стефана на поведінку магнітогідродинамічної (МГД) кассонового нанофлюїду через пористе середовище під час хімічної реакції. Ми також досліджуємо вплив параметрів випромінювання, Джоулевого тепла та розподілу швидкості за допомогою двофазної моделі для нанофлюїдів. Перетворення подібності можна використовувати для перетворення первинних диференціальних рівнянь із частинними похідними (PDE) у звичайні диференціальні рівняння (ODE). Для вирішення нелінійних рівнянь використано алгоритми MATLAB Shooting і Runge-Kutta. Варіації безрозмірних параметрів показують вплив на масообмін, тепло та властивості потоку рідини. Показано, що коефіцієнт поверхневого тертя зменшується зі збільшенням параметра S видування Стефана. Із збільшенням значень параметрів ковзання Томпсона і Трояна концентрація рідини зменшується. Зі збільшенням і k теплота рідини зростає, але її концентрація падає. Результати цього аналізу надають кілька привабливих аспектів, які дадуть можливості для подальшого вивчення проблем.

Ключові слова: *Кассон; хімічна реакція; МГД; пористий; випромінювання; Томпсон і Троян ковзання*